

# Comparison of the Spin Relaxation and Solution Dynamics of Poly(2-methyl-6-phenyl-1,4-phenylene oxide) with Those of Poly(2,6-dimethyl-1,4-phenylene oxide)

Ronald P. Lubianez, Alan Anthony Jones,\* and Michael Bisceglia

Jeppson Laboratory, Department of Chemistry, Clark University, Worcester, Massachusetts 01610. Received June 28, 1979

**ABSTRACT:** The spin-lattice relaxation times of the methyl protons of poly(2,6-dimethyl-1,4-phenylene oxide) ( $M_2$ PPO) and poly(2-methyl-6-phenyl-1,4-phenylene oxide) (MPHPPO) were measured for 20% (wt/wt) solutions of each polymer in  $CDCl_3$  as a function of molecular weight and temperature. The molecular weight dependence of  $T_1$  at a given temperature was interpreted with the Jones–Stockmayer specific motional model. Correlation times were obtained for three specific motions considered likely to occur in each polymer which contributes to the spin relaxation of the methyl protons. These motions are overall rotatory diffusion, three-bond crankshaft rearrangements, and anisotropic rotation of the backbone phenyl group. Methyl group rotation occurs too rapidly to effectively contribute to spin relaxation; however, it does partially average the dipole–dipole interactions. At high molecular weights, relaxation in both polymers is dominated by anisotropic phenyl group rotation characterized by correlation times from 0.2 to 0.4 ns for  $M_2$ PPO and from 0.2 to 0.7 ns for MPHPPO. The three-bond crankshaft rearrangements of the backbone are characterized by correlation times ranging from 2 to 13 ns for  $M_2$ PPO and 2 to 21 ns for MPHPPO. The apparent activation energy for the three-bond crankshaft motion is 29 kJ/mol in  $M_2$ PPO and 32 kJ/mol in MPHPPO. The apparent activation energy for backbone phenyl group rotation is 8 kJ/mol in  $M_2$ PPO and 16 kJ/mol in MPHPPO.

A recent nuclear spin relaxation study of local motion in poly(2,6-dimethyl-1,4-phenylene oxide) ( $M_2$ PPO) in solution<sup>1</sup> prompted this analogous study of poly(2-methyl-6-phenyl-1,4-phenylene oxide) (MPHPPO). In the case of  $M_2$ PPO, the interpretation indicated the local motion in this polymer differed substantially from most other polymers studied by NMR, such as polystyrene,<sup>2–5</sup> polyoxymethylene,<sup>6</sup> and polyisobutylene.<sup>7–10</sup> The oxygen linkages between phenylene units in the backbone allow facile phenyl group rotation, and indeed this rotation dominates spin relaxation in solution. These low barriers to internal rotation along with high degrees of intramolecular flexibility have been proposed as major factors in the superior impact properties exhibited by  $M_2$ PPO.<sup>11</sup> In order to gain greater insight into the molecular dynamics of the technologically important poly(phenylene oxides), the current investigation examines the effects on local motion of the addition of bulky pendant phenyl groups to the backbone phenylene units.

Nuclear magnetic relaxation was employed to probe the local motion in 20% (wt/wt) solutions of  $M_2$ PPO and MPHPPO. Specifically, the spin–lattice relaxation times of the methyl protons of both polymers were measured as a function of molecular weight at various temperatures. As in the initial study of  $M_2$ PPO,<sup>1</sup> the specific motional model of Jones and Stockmayer<sup>12</sup> is employed to interpret the relaxation data. The interpretation derived from the application of this model to proton relaxation in MPHPPO and the extension of certain physical assumptions to MPHPPO is checked by predicting the values of  $T_1$  and the NOE of  $^{13}C$  nuclei in MPHPPO for comparison with experimental values.

## Experimental Section

Five grams of high molecular weight MPHPPO was kindly provided by General Electric Research and Development Center in Schenectady, N.Y. This sample was fractionated from chloroform solution with methanol. Low molecular weight samples of MPHPPO were prepared according to the method of White and Klopfer<sup>13</sup> without modification and were also fractionated from chloroform solution with methanol.

Solution viscosities of both high and low molecular weight fractions were determined in chloroform at 25 °C with an Ubbelohde viscometer. The viscosity average molecular weights,  $M_v$ , were calculated from the intrinsic viscosities,  $[\eta]$ , according to the equation

$$[\eta] \text{ (dL/g)} = 1.57 \times 10^{-4} M_v^{0.69} \quad (1)$$

The Mark–Houwink parameters were obtained from a linear least-squares analysis of a double logarithmic plot of  $[\eta]$  vs.  $M_w$  for MPHPPO in chloroform at 25 °C.<sup>14</sup> The Huggins constant,  $k'$ , was determined from the concentration dependence of the specific viscosities of MPHPPO in chloroform at 25 °C. A plot of  $\ln(\eta_{sp}/c)$  vs.  $c$  for five concentrations ranging from 0.035 to 0.15 g/mL yielded a value of 0.58 for  $k'$ .

The fractionation of the high molecular weight lot yielded ten fractions with  $M_v$  ranging from  $1.5 \times 10^4$  to  $7.8 \times 10^4$ . The fractionation of a total of 6 g from two low molecular weight lots yielded seven fractions each with  $M_v$  ranging from  $4.3 \times 10^3$  to  $2.5 \times 10^4$ . The sample preparation and characterization of  $M_2$ PPO are described in detail elsewhere.<sup>1</sup>

The spin–lattice relaxation measurements on the methyl protons of MPHPPO were conducted at 30 MHz on degassed solutions of the respective polymers in chloroform-*d*. Two NMR spectrometers were used to accumulate the data. One instrumental system has been described elsewhere,<sup>1</sup> and the second system is a Bruker SXP20-100 variable field spectrometer operating at 30 MHz and interfaced to a Nicolet NMR-812 laboratory computer. Temperature control in the latter system was achieved with a Bruker B-ST 100/700 thermoregulator. Carbon-13 relaxation measurements were also conducted at 22.63 MHz on the Bruker SXP20-100 spectrometer. For both protons and carbon-13 nuclei, a standard  $180^\circ$ – $\tau$ – $90^\circ$  pulse sequence followed by Fourier transformation was used to monitor the return of the spin magnetizations to equilibrium. The  $^{13}C$  NOE measurements were conducted at 22.63 MHz, and the values were obtained by comparing the integrated peak intensities obtained under conditions of continuous broadband proton decoupling with the equilibrium integrated intensities obtained when the decoupler was gated on only during computer acquisition.

## Results

The return to equilibrium of the methyl proton magnetization in MPHPPO and  $M_2$ PPO is somewhat nonexponential, but as in the case of the methyl proton decay curves of the 5% (wt/wt) and 10% (wt/wt) solutions of  $M_2$ PPO,<sup>1</sup> the initial return to equilibrium is characterized by a single time constant. These earlier data on  $M_2$ PPO were successfully analyzed<sup>1</sup> by considering only the initial parts of the decay curves where the nonexponential effects are minimal, and the decay is apparently characterized by a single time constant. This approach will therefore now be used to analyze the methyl proton decay curves for the 20% (wt/wt) solutions of  $M_2$ PPO and MPHPPO. Spe-

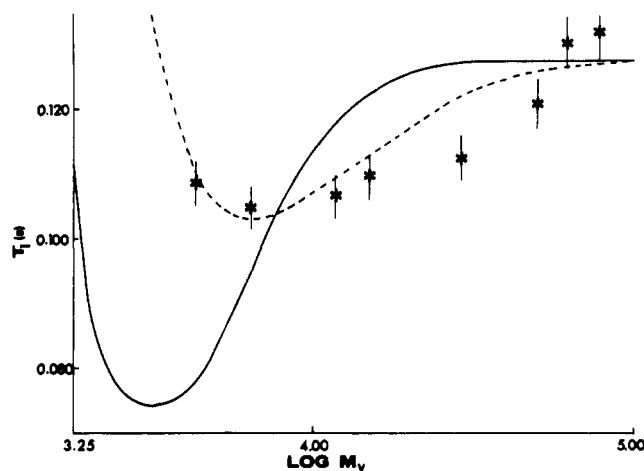


**Figure 1.** Methyl group proton spin-lattice relaxation time,  $T_1$ , as a function of molecular weight for 20% (wt/wt) solutions of MPhPPO in  $\text{CDCl}_3$  at 25 °C. The points are experimental data, and the dashed line is a simulation based on the specific motional model with the assumption of a polydispersity index of 1.5. The solid line is a prediction for monodisperse fractions based on the interpretation for polydisperse samples.

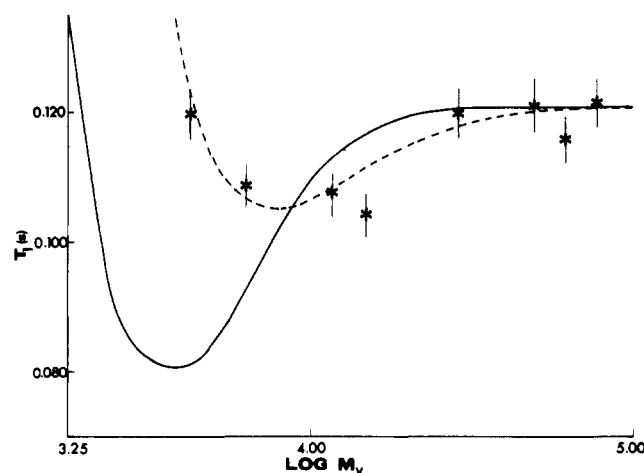


**Figure 2.** The same plot as Figure 1 but at 40 °C.

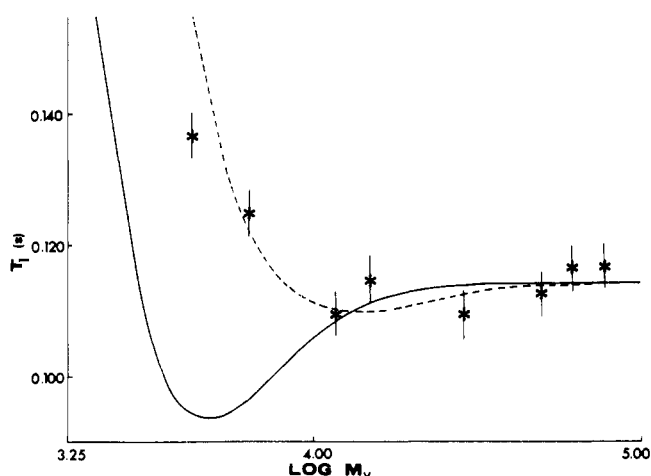


**Figure 3.** The same plot as Figure 1 but at 70 °C.

cifically in a plot of  $\ln(A_\infty - A\tau)$  vs.  $\tau$ , linear least-squares analysis yields the same value of  $T_1$  when delay times from  $\tau = 0$  to approximately  $\tau = T_1/2$  are considered. If delay times are beyond this range, a systematic increase in the slope is exhibited in all cases. Therefore, the methyl proton spin-lattice relaxation time,  $T_1$ , will be identified with the initial decay constant based on five to seven delay

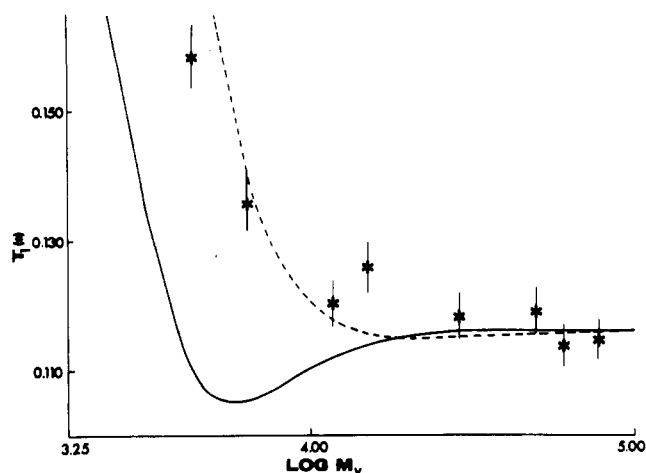


**Figure 4.** The same plot as Figure 1 but at 85 °C.

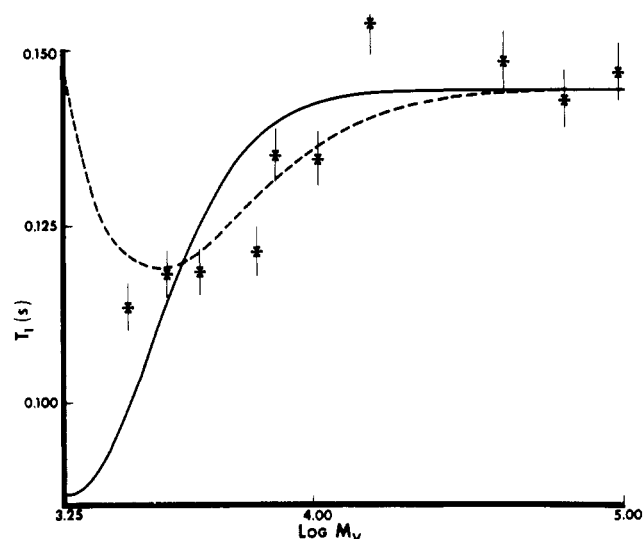


**Figure 5.** Methyl group proton spin-lattice relaxation time,  $T_1$ , as a function of molecular weight for 20% (wt/wt) solutions of  $\text{M}_2\text{PPO}$  in  $\text{CDCl}_3$  at 20 °C. See Figure 1 for the significance of the lines.

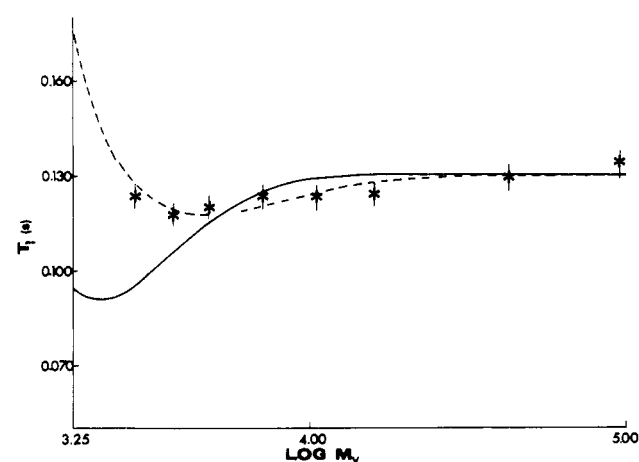


**Figure 6.** The same plot as Figure 5 but at 40 °C.

times in the range of 0 to approximately  $T_1/2$ .

The spin-lattice relaxation times of the methyl protons of 20% (wt/wt) solutions of MPhPPO were measured at 30 MHz as a function of the viscosity average molecular weight at four temperatures (25, 40, 70, and 85 °C) shown in Figures 1–4, respectively. The spin-lattice relaxation times of the methyl protons of 20% (wt/wt) solutions of

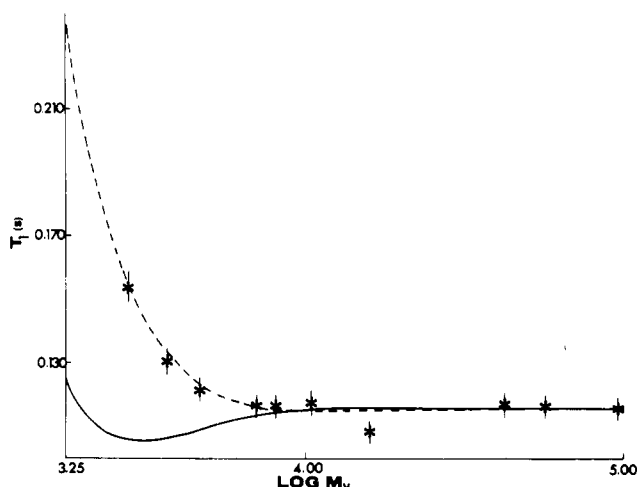


Figure 7. The same plot as Figure 5 but at 70 °C.

M<sub>2</sub>PPO were also measured at 30 MHz as a function of  $M_w$ . These latter measurements were conducted at three temperatures (20, 40, and 70 °C) shown in Figures 5–7.

The  $T_1$  minimum as a function of molecular weight exhibited in both sets of data at the lower temperatures diminishes systematically as the temperature is increased. Analogous behavior is encountered in the 10% (wt/wt) solutions of M<sub>2</sub>PPO.

Each  $T_1$  value on the plots is an average of two to four separate measurements of  $T_1$ , and it was determined that no systematic discrepancies were apparent in the data that were averaged from the two different spectrometers. The typical standard deviation is 3%, whereas the estimated accuracy of the averaged  $T_1$  values is 10%.

### Interpretation

The dominant source of relaxation for the methyl protons in MPhPPO and M<sub>2</sub>PPO<sup>1</sup> via the intramolecular dipole–dipole mechanism is with methyl protons on the same methyl group. The methyl–proton internuclear distance within a given methyl group is much shorter than any other proton internuclear distance in the repeat unit. This geometry favors intragroup relaxation since the dipolar mechanism is dependent on the inverse sixth power of the internuclear distance. Under these circumstances, the return to equilibrium of the longitudinal magnetization of the methyl protons is often characterized by a single rate constant; however, it is well known that the longitudinal magnetization of methyl protons may exhibit nonexponential behavior due to cross-correlation effects even when cross-relaxation is not significant.<sup>15–18</sup> Since the effects of cross-correlation are minimal at short delay times, the decay may be approximated by a single rate constant.<sup>15</sup> It is this initial rate of decay that is identified with  $T_1$  and subsequently with the spectral densities given by Solomon.<sup>19</sup>

$$1/T_1 = \sum_j (9/8) \gamma^4 \hbar^2 r_j^{-6} (J_1(\omega_H) + J_2(2\omega_H)) \quad (2)$$

The proton gyromagnetic ratio is denoted by  $\gamma$ , the Larmor frequency by  $\omega_H$ , and the internuclear separation in the methyl group by  $r$ . Through the above identification it is possible to characterize local motion in M<sub>2</sub>PPO and MPhPPO from the relaxation of the methyl spin system.

The phenyl protons, on the other hand, do not lend themselves to a simple treatment. The extremely nonexponential return to equilibrium of the longitudinal phenyl proton magnetization in M<sub>2</sub>PPO has been attributed to cross-relaxation with methyl protons on the same side of the backbone phenyl ring.<sup>20</sup> Since this mode of relaxation

does not provide an easily decipherable indication of the local motion in either MPhPPO or M<sub>2</sub>PPO, only the relaxation of the methyl protons in each system will serve as a probe of the local motion.

The specific motional model of Jones and Stockmayer<sup>12</sup> will be employed to interpret the methyl proton relaxation data as a function of molecular weight. This dynamic description considers three different types of motion that are likely to occur in a randomly coiled polymer molecule in solution: (1) overall rotatory diffusion, (2) backbone rearrangements caused by the three-bond motion, and (3) internal rotation relative to the backbone bonds. Each of these motions is considered as an independent source of motion modulating the dipole–dipole interaction.

Isotropic rotatory diffusion is described by an exponential correlation function characterized by the correlation time,  $\tau_0'$ , at infinite dilution.<sup>21,22</sup>

$$\tau_0' = 2M[\eta]\eta_0/3RT \quad (3)$$

The molecular weight is denoted by  $M$ , the intrinsic viscosity by  $[\eta]$ , and the viscosity of the solvent by  $\eta_0$ . In a solution of finite concentration, the correlation time characterizing isotropic rotatory diffusion,  $\tau_0$ , is estimated from eq 4, which is analogous to the Martin variation of the Huggins equation for specific viscosity.

$$\ln(\tau_0/\tau_0') = k[\eta]c \quad (4)$$

The distribution of correlation times for overall rotatory diffusion resulting from the distribution of molecular weights in polydisperse samples is accounted for by folding eq 4 with a Schulz–Zimm molecular weight distribution function.<sup>1</sup> Although the ratio of  $M_w/M_n$  is not known for samples of either polymer, a value of 1.5 was estimated in the previous NMR study of the same fractions of M<sub>2</sub>PPO.<sup>1</sup> In view of the similarities in synthesis, fractionation, and the range of fractions obtained, it is also reasonable to assume that  $M_w/M_n$  for MPhPPO is between 1.3 and 2.0, so a value of 1.5 will be used as an estimate of  $M_w/M_n$  for MPhPPO as well as M<sub>2</sub>PPO. The error associated with relying only on an estimate of  $M_w/M_n$  in the range of 1.3 to 2.0 is comparable to other errors involved in the simulation process.<sup>1</sup>

The second type of motion modulating the dipolar interaction is backbone rearrangement described presently by a three-bond jump in a chain lying on a tetrahedral lattice.<sup>23,24</sup> Although the requirement of tetrahedral bond angles is not strictly met in either PPO, the bond angle of about 120° between phenyl units is a reasonable approximation. The sharp cutoff formulation<sup>12</sup> of this lattice description of motion will be employed, and for a segment containing  $2m - 1$  bonds, the spectral density characterizing the motion of the central bond is given by<sup>12,25</sup>

$$J(\omega) = 2 \sum_{k=1}^s \frac{G_k \tau_k}{1 + \omega^2 \tau_k^2}$$

$$\tau_k^{-1} = \omega \lambda_k \quad s = (m + 1)/2$$

$$\lambda_k = 4 \sin^2((2k - 1)\pi/2(m + 1)) \quad (5)$$

$$G_k = 1/s + (2/s) \sum_{q=1}^{s-1} \exp(-\gamma q) \cos((2k - 1)\pi q/2s)$$

$$\gamma = \ln 9$$

The parameters in this component of the model are the rate of occurrence of the three-bond jump given by  $\omega$  and the extent of coupling given by either  $m$  or  $s$ . The distribution of correlation times,  $\tau_k$ , is conveniently summarized by a harmonic average,  $\tau_h$ .

$$\tau_h = \langle \tau_k^{-1} \rangle^{-1} \quad (6)$$

The value of  $\tau_h$  is equivalent to  $1/(2w)$  and provides a convenient means of associating a correlation time with the rate of backbone rearrangement.

The third type of motion considered is anisotropic internal rotation. Two types of internal rotation that modulate the dipolar interaction of methyl protons in  $M_2PPO$  and  $MPhPPO$  are conceivable. In each case there is phenyl group rotation about the  $C_1C_4$  axis and methyl group rotation about the threefold symmetry axis. It has been shown previously that methyl group rotation in  $M_2PPO$  occurs much too rapidly to significantly contribute to the relaxation; however, it does partially average the dipole-dipole interaction.<sup>1,26</sup> It is reasonable to expect rapid methyl group rotation in  $MPhPPO$  as well. For the second rotation a Woessner type description of anisotropic rotation<sup>27</sup> will be used to characterize phenyl group rotation as random jumps between two energetically equivalent equilibrium positions at a rate of  $(2\tau_{irp})^{-1}$ .<sup>1,28</sup>

The spectral density arising from the combination of isotropic rotatory diffusion, backbone rearrangements caused by the three-bond jump, anisotropic phenyl group rotation, and rapid methyl group rotation, assuming each motion is independent, is

$$J_i(\omega_i) = 2fK \sum_{k=1}^s G_k \left( \frac{A\tau_{k0}}{1 + \omega_i^2 \tau_{k0}^2} + \frac{B\tau_{bk0}}{1 + \omega_i^2 \tau_{bk0}^2} + \frac{C\tau_{k0}}{1 + \omega_i^2 \tau_{k0}^2} \right)$$

$$\tau_{bk0}^{-1} = \tau_0^{-1} + \tau_k^{-1} + \tau_{irp}^{-1} \quad \tau_{k0}^{-1} = \tau_0^{-1} + \tau_k^{-1}$$

$$A = (3 \cos^2 \Delta - 1)^2/4 \quad C = (3 \sin^4 \Delta)/4 \quad (7)$$

$$B = (3 \sin^2 2\Delta)/4 \quad f = (3 \cos^2 \alpha - 1)^2/4 = 1/4$$

$$K_0 = 4/5 \quad K_1 = 2/15 \quad K_2 = 8/15$$

The angle between the methyl group axis and the  $C_1C_4$  axis of the backbone phenyl group, denoted by  $\Delta$ , is  $60^\circ$  for  $M_2PPO$  and  $MPhPPO$ . The angle between the internuclear proton vector in the methyl group and the threefold symmetry axis, given by  $\alpha$ , is  $90^\circ$ .

The correlation times characterizing backbone rearrangements and phenyl group rotation in each polymer are determined by the use of eq 2 and 7 to simulate the molecular weight dependence of  $T_1$  at a given temperature. Results obtained previously on 20% (wt/wt) solutions of  $M_2PPO$  at  $20^\circ C$ <sup>1</sup> provided a convenient starting point for the adjustment of model parameters. It was found that coupling over five bonds in the backbone produced the best simulations for both polymers at all temperatures. The proton separation in a methyl group was set at 1.77 Å. The only parameters that changed as a function of temperature or molecule weight were  $\tau_{irp}$  and  $\tau_h$ . The simulations of  $T_1$  vs. molecular weight for  $MPhPPO$  are shown in Figures 5–7. The correlation times producing the dashed line simulations for polydisperse samples are given in Table I. The solid lines in each figure are predictions for monodisperse samples based on the correlation times obtained from the simulations of polydisperse samples.

The striking similarities in the shapes of the  $T_1$  vs. molecular weight curves for the two polymers are apparent. The presence of minima in these curves aided the choice of parameters for simulation as it did in the previous  $M_2PPO$  study.<sup>1</sup>

A test of the interpretational aspects of the  $MPhPPO$  study based on proton relaxation can be attempted by predicting the experimentally observed values of the carbon-13  $T_1$  and NOE of the C-3,5 phenyl carbons in the backbone, the relaxation of which is not obscured by

Table I  
Simulation Parameters Characterizing Local Motion  
in  $MPhPPO$  and  $M_2PPO$

concn, % (wt/wt) in $CDCl_3$	$T$ , $^\circ C$	$\tau_{irp}$ , ns	$\tau_h$ , ns	$2m - 1$	$T_1$ , s <sup>a</sup>
<b><math>MPhPPO</math></b>					
20	25	0.72	21	5	0.132
20	40	0.55	11	5	0.121
20	70	0.33	4.0	5	0.117
20	85	0.25	2.3	5	0.115
<b><math>M_2PPO</math></b>					
20	20	0.41	13	5	0.147
20	40	0.30	7.0	5	0.134
20	70	0.25	2.3	5	0.116

<sup>a</sup> High molecular weight limit.

correlation or cross-relaxation effects. The  $^{13}C$   $T_1$  and NOE which were measured at 22.63 MHz for a 20% (wt/wt) solution of high molecular weight  $MPhPPO$  in  $CDCl_3$  at  $40^\circ C$  are 0.069 and  $1.7 \pm 0.3$ , respectively. The respective predicted values based on correlation times obtained from proton relaxation are 0.075 and 2.0. The agreement between the observed and predicted values is well within the experimental uncertainties of the measurements and the simulation.<sup>1</sup> The agreement also supports the use of the model and the interpretation derived from the relaxation of the methyl protons.

## Discussion

The similarities of local motion in both  $MPhPPO$  and  $M_2PPO$  are revealed in this present interpretation. In both polymers, backbone rearrangement and phenyl group rotation in the backbone contribute to spin relaxation with the latter motion dominating. In fact the presence of minima in the molecular weight dependence of  $T_1$  for both polymers combined with the values of  $T_1$  in the high molecular weight limit indicate the dominance of phenyl group rotation. The time scales of the two distinct motions differ by approximately an order of magnitude in each polymer with phenyl group rotation being faster than segmental motion caused by the three-bond crankshaft-type motions. Both motions in  $MPhPPO$ , however, occur at slightly slower rates than those in  $M_2PPO$ . For instance the correlation times describing motion in  $MPhPPO$  at  $85^\circ C$  are identical with the times in  $M_2PPO$  at  $70^\circ C$ .

A concentration- and temperature-dependent study conducted previously on  $M_2PPO$ <sup>1</sup> indicated that the internal phenyl group rotation was independent of backbone rearrangement. An identical concentration study was not conducted on  $MPhPPO$  because of the temperature dependence; the differing time scales of motion and dynamic similarities indicate the likelihood of the independence of phenyl group rotation from backbone rearrangement. Apparent activation energies for backbone rearrangement and internal phenyl group rotation in  $MPhPPO$  were calculated from the appropriate values of  $\tau_h$  and  $\tau_{irp}$ , respectively, given in Table I. The corresponding Arrhenius plots shown in Figures 8 and 9 yield values of 32 kJ/mol for backbone rearrangements and 16 kJ/mol for phenyl group rotation. Similar plots for 20% (wt/wt) solutions of  $M_2PPO$  yield apparent activation energies of 29 kJ/mol for backbone rearrangement and 8 kJ/mol for phenyl group rotation.

Although the activation energies for segmental motion are identical within experimental error,  $MPhPPO$  exhibits a twofold increase in the barrier to backbone phenyl group rotation. Qualitatively it seems reasonable that the introduction of bulky pendant phenyl groups on the rotating

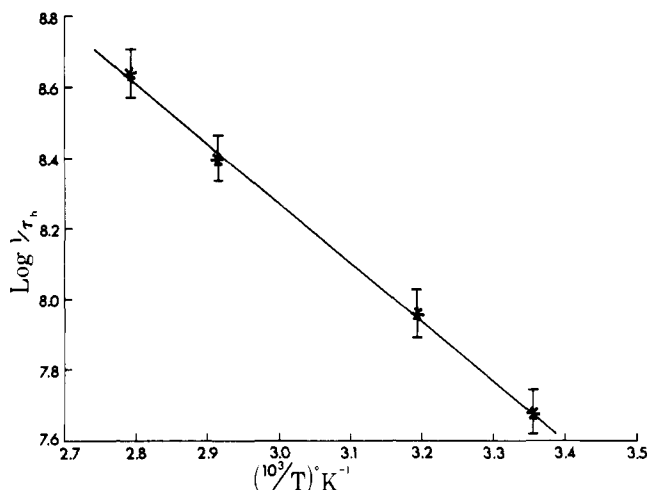


**Figure 8.** Logarithm of the inverse backbone correlation time,  $\tau_b$ , vs. inverse absolute temperature for 20% (wt/wt) solutions of MPhPPO in  $\text{CDCl}_3$ .

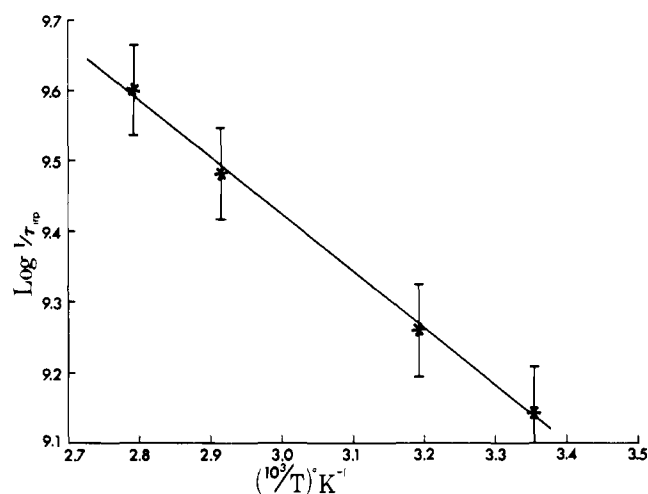


**Figure 9.** Logarithm of the inverse phenyl group rotational correlation time of the backbone phenyl unit,  $\tau_{ip}$ , vs. inverse absolute temperature for 20% (wt/wt) solutions of MPhPPO in  $\text{CDCl}_3$ .

units in MPhPPO would cause this increase. A semi-empirical calculation for an isolated chain indicates a very low barrier to backbone phenyl group rotation in  $\text{M}_2\text{PPO}$  and only a slightly higher barrier for MPhPPO. Although these low calculated barriers are in general agreement with the low activation energy for backbone phenyl group rotation, the activation energy for MPhPPO is quite a bit larger than that for  $\text{M}_2\text{PPO}$ . A dynamic mechanical study<sup>29</sup> on bulk PPO's showed no  $\beta$  peak from backbone phenyl group rotation in MPhPPO, although a distinct  $\beta$  peak was observed for  $\text{M}_2\text{PPO}$ . An intermolecular packing effect was suggested to account for the lack of a  $\beta$  peak in MPhPPO,<sup>29</sup> but the spin relaxation data in solution where intermolecular effects are reduced point to a higher barrier for backbone phenyl group rotation. Perhaps an increase in the intramolecular barrier contributes to the lack of a distinct  $\beta$  peak in MPhPPO by shifting it closer

to the glass transition. The lower glass transition temperature<sup>29</sup> of MPhPPO relative to  $\text{M}_2\text{PPO}$  increases the likelihood that the  $\beta$  relaxation might be overlapped. While dynamic descriptions developed from solution data do not necessarily extrapolate to the bulk, the higher activation energy for backbone phenyl group rotation in solution at least suggests the  $\beta$  relaxation in MPhPPO could be at higher temperatures in the vicinity of the glass transition.

**Acknowledgment.** The authors thank Drs. A. R. Schultz and D. M. White at the General Electric Research and Development Center in Schenectady, New York, for their cooperation in supplying materials for this study. The research was carried out with financial support of the National Science Foundation, Grant DMR 7716088, Polymers Program. This research was also supported in part by a National Science Foundation Equipment Grant No. CHE 77-09059.

## References and Notes

- (1) A. A. Jones and R. P. Lubianez, *Macromolecules*, **11**, 126 (1978).
- (2) A. Allerhand and R. K. Hailstone, *J. Chem. Phys.*, **56**, 3718 (1972).
- (3) J. Schaefer and D. F. S. Natusch, *Macromolecules*, **5**, 416 (1972).
- (4) A. A. Jones, K. Matsuo, K. F. Kuhlmann, F. Geny, and W. H. Stockmayer, *Polym. Prepr., Am. Chem. Soc., Div. Polym. Chem.*, **16**, 578 (1975).
- (5) K. Matsuo, K. F. Kuhlmann, N. W.-H. Yang, W. H. Stockmayer, F. Geny, and A. A. Jones, *J. Polym. Sci., Polym. Phys. Ed.*, **15**, 1347 (1977).
- (6) G. Hermann and G. Weil, *Macromolecules*, **8**, 171 (1975).
- (7) W. P. Slichter and D. D. Davis, *Macromolecules*, **1**, 47 (1968).
- (8) Y. Inoue, A. Nishioka, and R. Chujo, *J. Polym. Sci., Polym. Phys. Ed.*, **11**, 2237 (1973).
- (9) F. Heatley, *Polymer*, **16**, 443 (1975).
- (10) J. Spevacek and B. Schneider, *J. Polym. Sci., Polym. Phys. Ed.*, **14**, 1789 (1976).
- (11) A. E. Tonelli, *Macromolecules*, **5**, 558 (1972); **6**, 503 (1973).
- (12) A. A. Jones and W. H. Stockmayer, *J. Polym. Sci., Polym. Phys. Ed.*, **15**, 847 (1977).
- (13) D. M. White and A. J. Klopfer, *J. Polym. Sci., Part A-1*, **10**, 1565 (1972).
- (14) A. R. Shultz, *J. Polym. Sci., Part A-2*, **8**, 883 (1970).
- (15) L. G. Werbelow and A. G. Marshall, *J. Magn. Reson.*, **11**, 299 (1973).
- (16) L. G. Werbelow and A. G. Marshall, *J. Am. Chem. Soc.*, **95**, 5132 (1973).
- (17) L. G. Werbelow and D. M. Grant, *J. Chem. Phys.*, **63**, 544 (1975).
- (18) L. G. Werbelow and D. M. Grant, *J. Chem. Phys.*, **63**, 4742 (1975).
- (19) I. Solomon, *Phys. Rev.*, **99**, 559 (1955).
- (20) A. A. Jones, R. P. Lubianez, and S. L. Shostak, *Polym. Prepr., Am. Chem. Soc., Div. Polym. Chem.*, **19** (1), 470 (1978).
- (21) J. Riseman and J. G. Kirkwood, *J. Chem. Phys.*, **16**, 442 (1949).
- (22) A. Isihara, *Adv. Polym. Sci.*, **5**, 531 (1958).
- (23) B. Valeur, J.-P. Jarry, F. Geny, and L. Monnerie, *J. Polym. Sci., Polym. Phys. Ed.*, **13**, 667 (1975).
- (24) B. Valeur, L. Monnerie, and J.-P. Jarry, *J. Polym. Sci., Polym. Phys. Ed.*, **13**, 675 (1975).
- (25) A. A. Jones, Gary L. Robinson, and F. E. Gerr, *ACS Symp. Ser.*, **103**, 271 (1979).
- (26) A. G. Marshall, P. G. Schmidt, and B. D. Sykes, *Biochemistry*, **11**, 3875 (1972).
- (27) D. E. Woessner, *J. Chem. Phys.*, **36**, 1 (1962).
- (28) A. A. Jones, *J. Polym. Sci., Polym. Phys. Ed.*, **15**, 863 (1977).
- (29) A. Eisenberg and B. Cayrol, *J. Polym. Sci., Part C*, **35**, 129 (1971).